SINTERING OF $BaCe_{0.85}Y_{0.15}O_{3-\delta}$ WITH/WITHOUT $SrTiO_3$ DOPANT

F. Dynys[*], A. Sayir[*1] and P. J. Heimann[*2],

NASA Glenn Research Center[*]/ CWRU[1] /OAI[2]

21000 Brookpark Rd.

Cleveland, OH 44135 USA

ABSTRACT

The perovskite composition, $BaCe_{0.85}Y_{0.15}O_{3-\delta}$, displays excellent protonic conduction at high temperatures making it a desirable candidate for hydrogen separation membranes. This paper reports on the sintering behavior of $BaCe_{0.85}Y_{0.15}O_{3-\delta}$ powders doped with $SrTiO_3$. Two methods were used to synthesize $BaCe_{0.85}Y_{0.15}O_{3-\delta}$ powders: (1) solid state reaction and (2) wet chemical co-precipitation. Co-precipitated powder crystallized into the perovskite phase at 1000 °C for 4 hrs. Complete reaction and crystallization of the perovskite phase by solid state was achieved by calcining at 1200 °C for 24 hrs. Solid state synthesis produce a coarser powder with a average particle size of 1.3 µm and surface area of 0.74 m^2/g. Co-precipitation produced a finer powder with a average particle size of 65 nm and surface area of 14.9 m^2/g. Powders were doped with 1, 2, 5 and 10 mole % $SrTiO_3$. Samples were sintered at 1450 °C, 1550 °C and 1650 °C. $SrTiO_3$ enhances sintering, optimal dopant level is different for powders synthesized by solid state and co-precipitation . Both powders exhibit similar grain growth behavior. Dopant levels of 5 and 10 mole % $SrTiO_3$ significantly enhances the grain size.

INTRODUCTION

The initial pathway for efficient hydrogen production to meet demand from the growing energy sector will come from the existing fossil fuels. To foster the initial growth of a localized distribution, small reformers and electrolyzers will provide on-site hydrogen generation. Reformers based on ceramic membrane technology potentially offer hydrogen production that is comparable to the cost of fossil fuels.

Protonic conducting ceramic with the chemical formula ABO_3 offers the promise of highly selective hydrogen separation at intermediate temperature (400-800°C). Among different perovskite-type oxides, barium cerates show promising high protonic conductivity but strong resistance to densification.[1,2] The solid state reaction of barium carbonate with ceria is ~~highly~~ utilized to synthesize $BaCeO_3$ base powders. The reaction is simple and there are no metastable products. Downside to the solid state process is the formation of large particles, high degree of agglomeration, possible inhomogeneities in chemical composition and contamination by the attrition steps. These powder characteristics negatively impact the sintering behavior. The use of excess barium enhances densification but its environmental reaction with CO_2 causes mechanical integrity problems.[3] Particle size reduction and cation doping are traditional methods to enhance sintering. Both approaches are used to investigate the sintering behavior of $BaCe_{0.85}Y_{0.15}O_{3-\delta}$.

Preliminary results on the sintering behavior of $SrTiO_3$ doped $BaCe_{0.85}Y_{0.15}O_{3-\delta}$ powders is reported. Two different synthesis methods were used to fabricate $BaCe_{0.85}Y_{0.15}O_{3-\delta}$ powder: (1) solid state reaction and (2) wet chemical co-precipitation utilizing ammonia/ammonium carbonate.[4,5]

EXPERIMENTAL PROCEDURE

Solid state (SS) synthesis was performed by mixing stoichiometric quantities of $BaCO_3$, CeO_2 and Y_2O_3 to yield the composition of $BaCe_{0.85}Y_{0.15}O_{3-\delta}$. The mixture was wet ball milled in alcohol for a period of 48 hrs to enhance homogeneity. The perovskite phase was synthesized by triple calcining: 800 °C for 6 hrs., 1000 °C for 10 hrs and 1200 °C for 24 hrs in Al_2O_3 crucibles. Calcined material was ground in a mortar and pestle to break up agglomerates between calcinations. The crystalline $BaCe_{0.85}Y_{0.15}O_{3-\delta}$ powder was doped with 1, 2, 5 and 10 mole % $SrTiO_3$ powder. The powders were wet ball milled for 24 hrs. to ensure $SrTiO_3$ homogeneity and break down of agglomerates.

Metal salts of $Ba(NO_3)_2$, $Ce(NO_3)_3 \cdot 6H_2O$ and $Y(NO_3)_3 \cdot xH_2O$ were used as precursors. The stoichiometric quantities were dissolved in deionized water at a ratio of 12 ml of water per gram of metallic salt to yield the composition of $BaCe_{0.85}Y_{0.15}O_{3-\delta}$. A precipitant solution was prepared by using a molar ratio of 1:2 of $(NH_4)_2CO_3$ to NH_4OH (28-30.0% aqueous solution). The molar ratio of $(NH_4)_2CO_3$ to $Ba(NO_3)_2$ and H_2O to $(NH_4)_2CO_3$ was held constant at 3 and 119, respectively. Mixed nitrate solution was dripped into a stirred base solution at 2 ml/min using an auto-titrator. Co-precipitation (COP) occurred instantaneously. The precipitate was separated from the solution by filtration and then freeze dried. The perovskite phase was synthesized by calcining at 1000 °C for 4 hrs in Al_2O_3 crucibles. The crystalline $BaCe_{0.85}Y_{0.15}O_{3-\delta}$ powder was doped with 1, 2, 5 and 10 mole % $SrTiO_3$ powder. The powders were wet ball milled for 24 hrs. to ensure $SrTiO_3$ homogeneity and break down of agglomerates.

Green pellets were pressed at 200 MPa using 2 grams of powder in a 15 mm die. Pellets were sintered in air at 1450 °C, 1550 °C and 1650 °C using a heating rate of 5 °C/min. A thin layer of $BaCe_{0.85}Y_{0.15}O_{3-\delta}$ powder was placed between the sample and Al_2O_3 crucible to abate the reaction between the crucible and sample. The densities of sintered pellets were determined by geometrical measurements and mass. Sample cross-sections were polished and etched to reveal the microstructure. Microstructures were examined with an Hitachi S-4700 scanning electron microscope (SEM). The grain size was determined by a linear intercept method.

The surface area of the synthesized powders were measured by nitrogen gas adsorption and analyzed using the 5 point Brunauer-Emmett-Teller method.

The amorphous and crystalline structures were characterized by x-ray diffraction. The x-ray diffractometer was equipped with a Cu K_α source with a wavelength of 0.1540 nm. The operating conditions were 45 KV and 40 mA. Scans were conducted at 3°/min with a sampling interval of 0.02°.

RESULTS AND DISCUSSION

X-ray diffraction (XRD) of the calcined powders is shown in Figure 1. The calcination temperatures used for each synthesis method was sufficient to produce crystalline perovskite powder of $BaCe_{0.85}Y_{0.15}O_{3-\delta}$. The measured surface area of the synthesized powders by SS and COP were 0.74 m^2/g and 14.9 m^2/g, respectively. Figure 2 shows a SEM micrograph of the SS synthesized $BaCe_{0.85}Y_{0.15}O_{3-\delta}$ powder. The particles are irregular shaped and size ranges from 1-5 μm. Average spherical particle diameter calculated from the surface area measurement is 1.3 μm. Grain boundaries are observed on the particle surfaces suggesting that particles are polycrystalline with sub-micron size grains. Figure 3 shows a SEM micrograph of the calcined co-precipitated powder. The powder is highly agglomerated and consists of particles that are

approximately 100 nm in size. The calculated average spherical particle size from the measured surface area is 65 nm and correlates well with the SEM observations.

Figure 4 shows the sintered density of $BaCe_{0.85}Y_{0.15}O_{3-\delta}$ as a function of $SrTiO_3$ content for

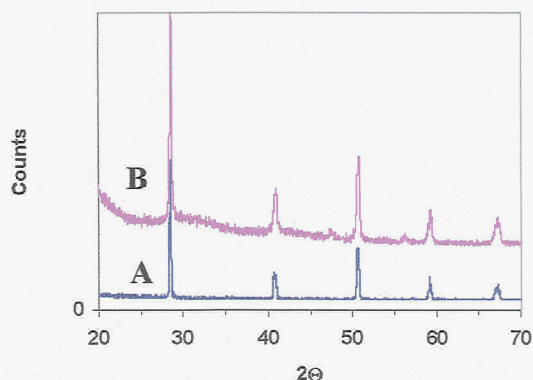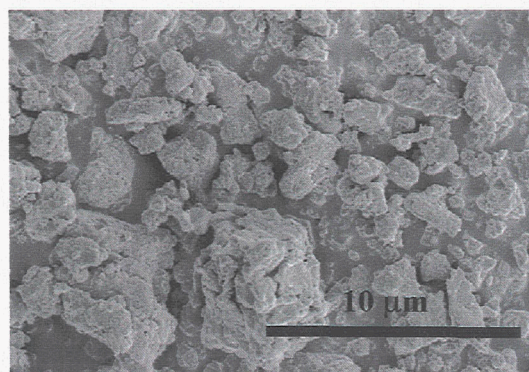Figure 1. XRD of $BaCe_{0.85}Y_{0.15}O_{3-\delta}$ (A) SS synthesis and (B) COP synthesis.

Figure 2. $BaCe_{0.85}Y_{0.15}O_{3-\delta}$ powder synthesized by SS.

powders synthesized by the SS method. The general trend is that $SrTiO_3$ doping enhanced the sintered density compared to the undoped samples. A 12% improvement in sintered density is observed at 1550 °C and 5.5% at 1650 °C. $SrTiO_3$ appears to be ineffective at 1450 °C. Figure 4 also illustrates that the sintering temperature was more effective in enhancing the sintered density than $SrTiO_3$ doping. Figure 5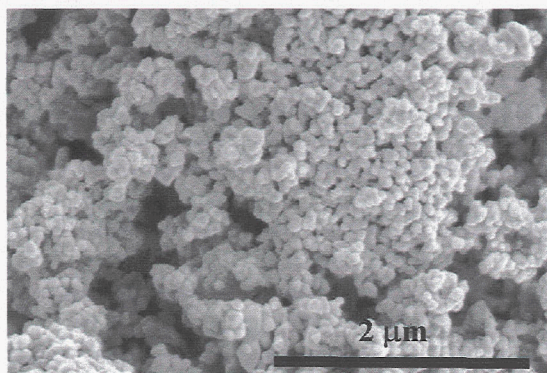 compares the sintered microstructures at 1650 °C for undoped $BaCe_{0.85}Y_{0.15}O_{3-\delta}$ and 10 mole % $SrTiO_3$ doped $BaCe_{0.85}Y_{0.15}O_{3-\delta}$. The roughness observed within grains in Figure 5 is caused by the preferential etching along crystallographic directions. A larger grain size is observed with the $SrTiO_3$ doping. Table I summarizes the average grain size of SS samples sintered at 1650 °C for $SrTiO_3$ dopant levels of 1 to 10 mole %. The average grain size for the undoped sample is 4 μm, showing very little grain growth when considering the starting particle size. Significant grain size enhancement is observed at 5 and 10 mole % $SrTiO_3$, average grain size of 5.5 μm and 9.4 μm are observed, respectively. In addition, the observed grain size distribution is narrow at 0, 1, 2 and 5 mole % $SrTiO_3$, it significantly broadens at 10 mole %.

Figure 6 shows the sintered density of $BaCe_{0.85}Y_{0.15}O_{3-\delta}$ as a function of $SrTiO_3$ content for powders synthesized by the COP method. The observed sintering behavior is significantly different than the SS samples. The sample sintered at 1650 °C with 10 mole % $SrTiO_3$

Figure 3. $BaCe_{0.85}Y_{0.15}O_{3-\delta}$ powder synthesized by COP.

Table I

Average Grain Size at 1650 °C

Mole % SrTiO₃	Ave. GS (μm) SS	Ave. GS (μm) COP
0	4.0	1.6
1	4.6	1.8
2	4.1	2.5
5	5.5	5.7
10	9.4	12

showed exceptional bloating, surface bubbles were observed on the surface. The general trend at 1550 °C and 1650 °C is that 1 to 2 mole % $SrTiO_3$ is optimal for sintered density, 5 and 10 mole % caused a reduction. The 1450 °C isotherm behaves similar to the SS material; increasing $SrTiO_3$ content enhances sintered density. The density increased by 19% at 10 mole % at 1450 °C. At 1 mole %, a 11% increased in density is observed at 1550 °C and 1650 °C. The sintered density of the COP samples show a larger dependence upon $SrTiO_3$ doping than upon temperature, opposite to what was observed for the SS samples. Figure 7 compares the sintered microstructures at 1650 °C for undoped $BaCe_{0.85}Y_{0.15}O_{3-\delta}$ and 10 mole % $SrTiO_3$ doped $BaCe_{0.85}Y_{0.15}O_{3-\delta}$. Large pores, >10 μm, are observed in the microstructure at 10 mole % $SrTiO_3$. Pore clusters are observed in the undoped sample which can be attributed to agglomeration problem. These large pores and pore clusters are responsible for low sintered densities. Table I shows the average grain for COP material sintered at 1650 °C. All dopant levels of $SrTiO_3$ show enhanced grain size. Significant grain growth occurred at 10 mole % $SrTiO_3$ along with significant broadening of the distribution. The COP grain growth behavior is similar to the SS material.
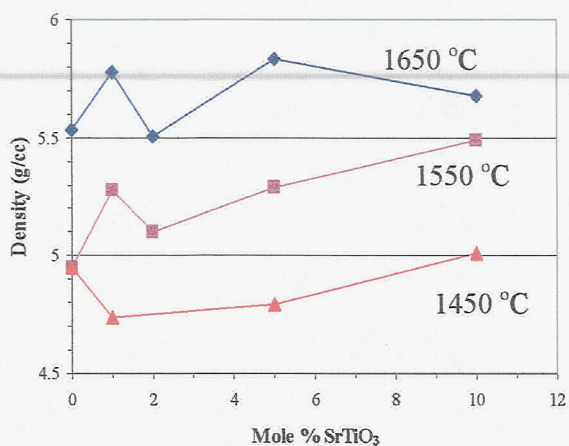

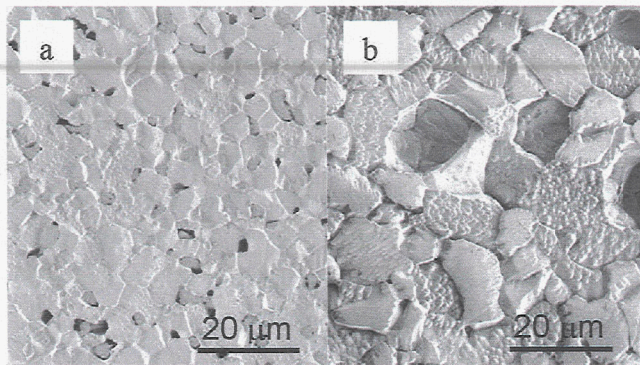Figure 4. Affect of $SrTiO_3$ on sintered density of SS derived powder.

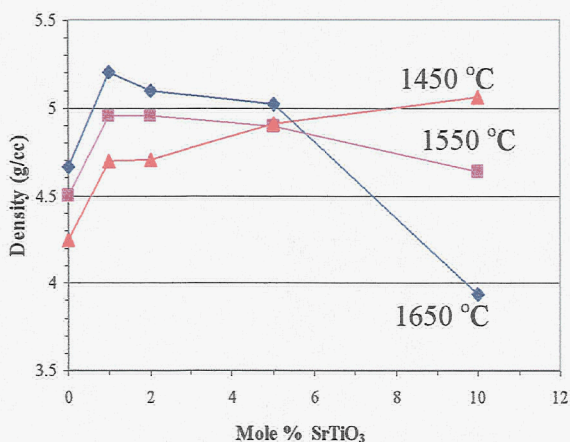Figure 5. Microstructure of SS derived powder sintered at 1650 °C :(a) undoped and (b) 10 mole % $SrTiO_3$.

Figure 6. Affect of $SrTiO_3$ on sintered density of COP derived powder.
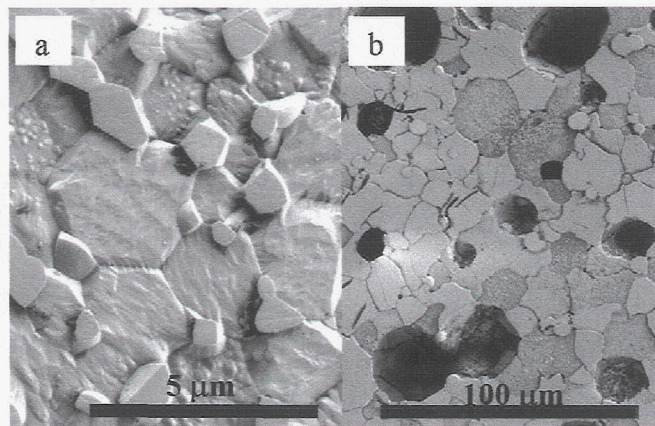

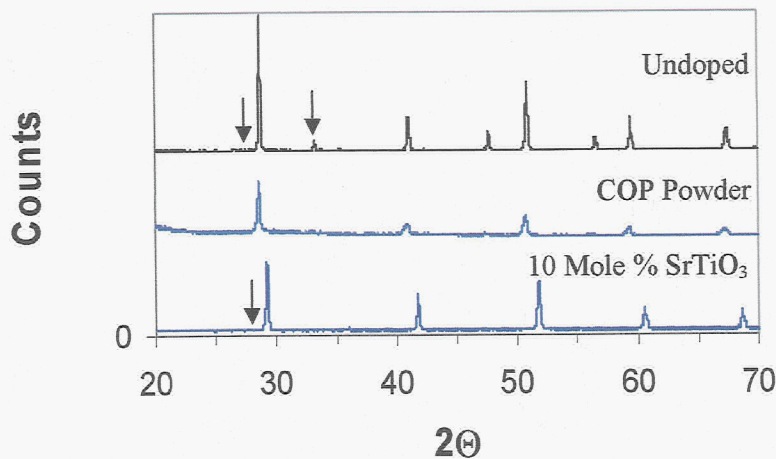Figure 7. Microstructure of COP derived powder sintered at 1650 °C :(a) undoped and (b) 10 mole % $SrTiO_3$.
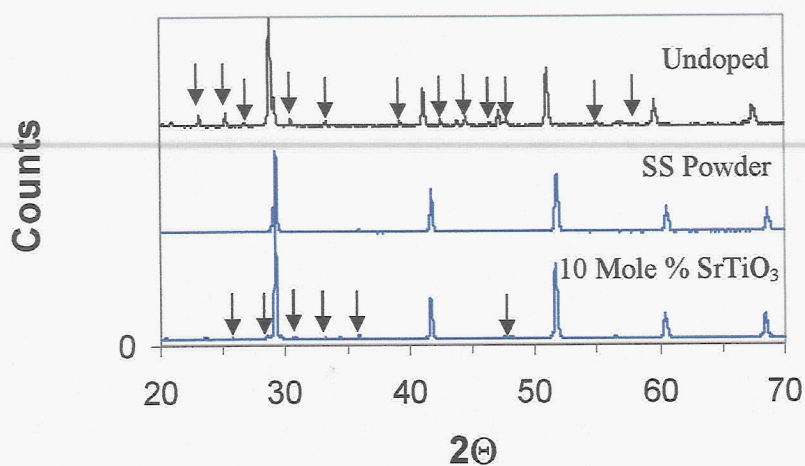
Figure 8. XRD of COP samples sintered at 1650 °C

Figure 9. XRD of SS samples sintered at 1650 °C

The surfaces of the sintered samples were analyzed for phases using XRD. Figures 8 and 9 show the XRD patterns for undoped and 10 mole % $SrTiO_3$ doped samples sintered at 1650 °C for COP and SS derived powders, respectively. Both figures contained the XRD of the undoped calcined powders for comparison. The doped and undoped samples do not maintain phase purity after sintering at 1650 °C. The arrows in Figures 8 and 9 indicate peaks due to secondary phase formation. For both powders, XRD indicates that the $SrTiO_3$ goes into solid solution as indicated by the shift in the perovskite peaks. Secondary phase formation is stronger in the SS samples than COP samples. One and two unknown diffraction peaks are observed in the COP samples. A large number of unknown diffraction peaks are observed in the SS samples. The severity of unknown diffraction peaks is more pronounced in the undoped sample than the $SrTiO_3$ doped sample. The unknown diffraction peaks do not correspond to Y_2O_3, CeO_2, $BaCO_3$ and BaO. For each isotherm, the SS and COP samples were sintered together. Contamination from sintering process appears minimal since the COP samples exhibit a few unknown diffraction peaks. Mixed CeO_2 phases were reported in sintered samples by Ma et al.[5] for Ba deficient $BaCe_{0.9}Y_{0.1}O_{3-\delta}$. Ma reported no additional phases in sintered samples with excess Ba. $BaZrO_3$ exhibits similar behavior as reported by Snijkers et al.[6] Both Ma and Snijkers attribute barium loss during sintering for secondary phase formation. Takeuchi et al.[8] have shown that phase transitions occur in Y-doped $BaCeO_3$. Crystal structure is dependent upon Y concentration and annealing atmosphere. Multi-phase materials were observed in atmospheres containing H_2 or H_2O. Calculated XRD from Takeuchi neutron diffraction data does not account for all the extra diffraction peaks. Further characterization is needed to identify the secondary phases.

There is insufficient data to elucidate the difference in sintering behavior between the $SrTiO_3$ doped SS and COP powders. It is suspected that sinter samples that exhibit bloating was caused by gas evolution in combination with a liquid phase. The roundness of the grain edges and boundary curvatures suggest liquid phase but it is undetectable in the SEM work. It is well

known that CeO_2 becomes oxygen deficient upon heating $\geq 1200\ ^\circ C$: $CeO_2 \rightarrow CeO_{1.83} \rightarrow CeO_{1.72} \rightarrow Ce_2O_3$. It can be postulated that the reaction of $SrTiO_3$ with $BaCeO_3$ results in the reduction of ceria. More work is needed to understand the material interactions during sintering.

SUMMARY

$BaCe_{0.85}Y_{0.15}O_{3-\delta}$ powders were synthesize by two methods: (1) solid state reaction and (2) wet chemical co-precipitation. Co-precipitation produces a finer particle size and reduces the calcination temperature and time to crystallize the perovskite structure. A 1000 $^\circ C$ calcination for 4 hrs. produce an average particle size of 65 nm. Solid state synthesis required multiple calcinations up to 1200 $^\circ C$ for 24 hrs. with an average particle size of 1.3 μm. Powders were doped with 1, 2, 5 and 10 mole % $SrTiO_3$. Samples were sintered at 1450 $^\circ C$, 1550 $^\circ C$ and 1650 $^\circ C$. $SrTiO_3$ doping was found to enhance sintering. However, the SS and COP doped powders exhibit different sintering behavior. Both powders exhibit similar grain growth behavior with $SrTiO_3$ doping. Dopant levels of 5 and 10 mole % $SrTiO_3$ significantly enhances the grain size.

ACKNOWLEDGEMENT

REFERENCES

1. K.D. Kreuer, An. Rev. of Mat. Res., **33**, 333, 2003.
2. A.S. Nowick, Y. Du and K.C. Liang. Solid State Ionics, **125**, 303, 1999
3. D. Shima & S. Haile, Solid State Ionics, **97**, 443, 1997
4. F. Boschini et al., J. Eur. Cer. Soc., **23**, 3035, 2003
5. J. Brzezińska-Miecznik, Mat. Letters, **56**, 273, 2002.
6. G. Ma et al., Solid State Ionics, **110**, 103, 1998.
7. F. Snijkers et al., Scripta Mat., **50**, 655, 2004.
8. K. Takeuchi et al., Solid State Ionics, **138**, 63, 2000.